Fluid Phase Equilibria 291 (2010) 81–89

Contents lists available at ScienceDirect

Fluid Phase Equilibria

journal homepage: www.elsevier.com/locate/fluid

Molecular force field investigation for Sulfur Hexafluoride: A computer simulation study

D. Dellis, J. Samios*

Department of Chemistry, Laboratory of Physical Chemistry, University of Athens, Panepistimiopolis 15771, Athens, Greece

ARTICLE INFO

Article history:
Received 21 January 2009
Received in revised form
14 December 2009
Accepted 17 December 2009
Available online 4 January 2010

SF_6 forcefield
Forcefield optimization

ABSTRACT

Force fields for Sulfur Hexafluoride (SF_6) from the literature, were investigated by means of their ability to reproduce experimental data in a wide range of thermodynamic conditions, including liquid, gas, vapor–liquid coexistence curve as well as supercritical states. Experimental data include numerous PVT state points, corresponding structural properties in terms of radial distribution functions, diffusion coefficient and shear viscosity. The existing force fields were extensively examined in the framework of molecular dynamics simulations and it is found that they do not accurately reproduce the macroscopic properties of the fluid, especially at high densities. To overcome this problem with the aim to obtain improved potential parameters that better reproduce experimental data, a multi-variable optimization of the force field parameters procedure has been systematically applied based on the "Simplex" method. Finally, it is found that for some common functional forms of these force fields, the new optimized parameters predict better the experimental properties of SF_6 under investigation compared to the original ones.

1. Introduction

Sulfur Hexafluoride (SF_6) is an octahedral molecule of O_h symmetry used in a wide range of applications. Due to the importance of this molecular system, numerous experimental and theoretical studies have been devoted so far to its properties at different conditions [1–19].

By carefully inspecting these previous studies, one sees that among them substantial efforts have focused on investigating the intermolecular interactions of the fluid and as a result some different potential models were proposed. From these potential models, we investigated those that have a common functional form and can be combined with potential models for other species. At this point, we mention that the first published and most used intermolecular interaction potential is a six-site rigid model proposed by Pawley [3]. Further to this, Kinney et al. [14] and Strauss et al. [13] proposed rigid seven-site potentials including electrostatic interactions. Finally, Olivet et al. [19] published quite recently a new potential model taking into account the intramolecular flexibility of the molecules.

According to the results obtained based on the aforementioned models, we may observe that the reliability of these potentials to describe successfully some properties of SF_6 is different from one model to another as well as restricted to some PVT thermodynamic state points. Concretely speaking, the potential model proposed by Pawley has been proposed to describe the plastic phase of SF_6. On the other hand, Kinney's potential proposed to describe freezing of SF_6 molecular clusters at low temperatures up to 200 K, while the Strauss's model to describe high pressure experimental neutron diffraction data at 398 K. Finally, the potential parameters proposed by Olivet were estimated to describe vapor pressure, saturated liquid density and surface tension of the fluid at two different isotherms, 260 and 290 K, two single states at 250 and 340 K, respectively, and shear viscosity at 333.15 and 350 K. It is quite clear that due to the relatively limited PVT phase space basis of these potentials, they yield to a higher or lower degree realistic results for properties of the molecular system. Investigation of these potential models shows that they do not adequately predict simple properties like pressure at low temperatures–high density region and some of these at temperatures close to the critical temperature.

Therefore, a systematic readjustment of the parameters of these models seems to be undoubtedly needed to describe the fluid at a wide region of PVT phase space including liquid, gas, supercritical states as well as the liquid–vapor coexistence curve. This is the main purpose of the present simulation study realized on the basis of an optimization procedure summarized in the next sections. The optimized potential models obtained are employed in extended molecular dynamics simulations (MD) of the system to calculate properties of interest. Finally, all the existing and optimized potential models proposed in this work are compared and their accuracy to predict certain properties of SF_6 has been discussed.

* Corresponding author. Tel.: +30 2107274534.
E-mail address: isamios@chem.uoa.gr (J. Samios).

0378-3812/$ – see front matter © 2009 Elsevier B.V. All rights reserved.
doi:10.1016/j.fluid.2009.12.018

Table 1
Potential models parameters of SF_6 from literature and obtained in this work.

Potential model	ϵ_F/k_B [K]	σ_F [Å]	ϵ_S/k_B [K]	σ_S [Å]	q_F −e−	ℓ_{S-F} [Å]	
Pawley [3]	70.60	2.700	–	–	0	1.565	–
Pawley Optimized	69.82	2.809	–	–	0	1.565	–
Strauss [13]	30.07	3.300	90.20	3.700	−0.110	1.564	LB
Strauss Optimized	27.02	2.947	165.14	3.228	−0.110	1.564	LB
Kinney [14]	26.27	2.943	151.54	3.405	−0.175	1.561	GM
Kinney Optimized	26.68	2.963	157.33	3.268	−0.175	1.561	GM
7Sites [This Work]	27.24	2.954	163.89	3.246	0	1.565	LB
Olivet [19]	73.13	2.760	–	–	0	1.565	LB
Olivet Optimized	69.82	2.809	–	–	0	1.565	LB
	$K_r = 693.48$ kJ/mol Å^2, $r_0 = 1.565$ Å $K_\theta = 307.36$ kJ/mol rad^2, $\theta_0 = 90^\circ$						
Spherical [This Work]		ϵ/k_B [K]		σ [Å]			
		238.89		4.615			

LB: Lorentz–Berthelot, GM: Geometric Mean.

2. Potential models

The potential models for SF_6 reported so far include mainly van der Waals type interactions in the form of Lennard–Jones potential, and in some cases also electrostatic interactions. Note also that in a recent treatment of Olivet [19] the corresponding proposed potential includes bond and angle vibrations. The rigid potential models use site–site interactions of the form:

$$U_{\alpha\beta} = \sum_{i=1}^{NS_\alpha}\sum_{j=1}^{NS_\beta} 4\epsilon_{ij}\left[\left(\frac{\sigma_{ij}}{r_{ij}}\right)^{12} - \left(\frac{\sigma_{ij}}{r_{ij}}\right)^{6}\right] + \frac{1}{4\pi\epsilon_0}\frac{q_i q_j}{r_{ij}} \quad (1)$$

where $U_{\alpha\beta}$ is the interaction energy between molecules α and β, NS is the number of sites, q_i the charge of atom i and σ_{ij}, ϵ_{ij} are the Lennard–Jones parameters for the interaction of site i with site j. The rigid potential models differ in parameters ϵ, σ and q as well as in the combination rule used to describe unlike site–site interactions. Pawley's model includes van der Waals type interactions only between F atoms. Strauss's [13] potential model includes van der Waals plus electrostatic interactions where the cross-interaction potential parameters among the atoms S and F from different molecules are defined by using the well known Lorentz–Berthelot combination rules. Kinney's model differs from that of Strauss as for the interaction between the atoms F and S where the author used the geometric mean for both ϵ and σ potential parameters and partial charges. Finally, the potential due to the Olivet includes, in addition to Pawley's rigid functional form, bond and angle vibrations described by a harmonic type potential

Table 2
Selected PVT state points from experiment [32] and this MD study using original and optimized potential models for SF_6 at four isotherms. The second line in simulated pressure, when present, correspond to the original model parameters prediction.

V_m [cm^3/mol]	P_{exp}	P_{sim} [bar]					
		Spherical	7 Sites	Pawley	Olivet	Strauss	Kinney
				235 K			
80.438	50	113.6±42	38.4±70	42.9±81	35.2±341	37.9±85	51.0±85
				−19.0±91	−146.6±300	819.0±435	−108.01±84
78.764	130	166.9±44	116.7±73	123.3±97	126.1±300	116.4±94	134.6±90
				26.7±96	−96.4±348	1250.4±657	−32.3±85
				298 K			
879.240	20	21.5±1	20.7±2	20.5±3	19.3±36	21.1±2	21.0±3
				22.1±3	20.3±26	16.1±3	20.1±3
651.450	23.57	26.2±2	24.7±4	24.6±4	23.1±35	25.3±4	24.8±5
				27.1±4	24.4±36	16.1±6	23.40±5
98.170	80	98.3±34	78.1±43	90.8±76	84.1±277	84.5±72	100.8±71
				106.4±77	106.5±265	319.9±79	11.3±70
90.300	200	190.4±41	198.8±52	214.8±82	186.3±331	203.5±84	209.6±85
				190.5±84	125.6±306	847.3±99	96.9±80
81.120	550	427.3±48	548.2±101	583.4±110	560.1±366	542.7±101	571.8±99
				437.5±102	382.2±354	2296.7±127	390.4±98
				350 K			
606.410	35	36.6±2	35.7±5	33.9±5	35.0±39	36.2±5	37.0±5
				38.4±5	34.3±52	27.8±6	34.5±6
130.780	100	102.2±25	101.7±49	104.0±54	91.8±216	101.9±52	102.8±50
				134.4±50	125.3±248	57.2±56	65.1±52
89.869	500	396.5±47	513.0±99	538.3±110	503.3±344	508.2±87	517.2±91
				474.0±96	309.2±299	1386.7±113	401.1±94
				398 K			
332.530	70	70.7±7	71.3±13	77.0±77	69.7±105	73.0±13	72.5±14
				80.0±13	70.0±104	52.5±15	67.7±14
175.750	120	117.04±19	123.4±35	121.6±35	124.1±173	112.7±34	123.3±35
				145.5±34	209.5±216	66.3±39	106.5±35
96.190	550	430.94±44	565.6±93	584.0±145	585.1±348	564.0±91	573.9±87
				548.7±95	521.0±302	1159.6±110	473.9±90

as follows:

$$U_{intra} = \sum_{bonds} K_r(r - r_0)^2 + \sum_{angles} K_\theta\left(\theta - \theta_0\right)^2 \quad (2)$$

where r_0 and θ_0 are the $S-F$ bond and $F-S-F$ angle equilibrium averages respectively. The details of the potential models are summarized in Table 1.

Table 2.

3. Force field optimization

In the force field optimization procedure applied in the present study, we have used PVT state points of SF_6 corresponding to four different isotherms. The set of these PVT state points at the low temperature of 235 K belongs to the liquid state. The state points at the isotherm of 398 K belong to the supercritical state, as this temperature is well above the critical one ($T_c = 318.7$ K). Finally, the two other isotherms of PVT data used have been selected to take into account the behavior of the phase diagram of the fluid near the critical temperature and close to the liquid–gas coexistence curve. So, we selected to study the isotherms at 298 and 350 K that is below and above the critical temperature, respectively. Note that, especially the isotherm slightly over the critical temperature exhibits some characteristic behavior that is of significant importance for a successful estimation of both ϵ and σ potential parameters. The optimization procedure includes the minimization over the van der Waals parameters ϵ and σ of the dimensionless quantity,

$$\mathcal{F}(\epsilon, \sigma) = \frac{1}{N}\sum_{i=1}^{N}\left(\frac{P_i^{sim}(\epsilon, \sigma) - P_i^{exp}}{P_i^{exp}}\right)^2 \quad (3)$$

where N is the number of PVT state points, P_i^{exp} the experimental and $P_i^{sim}(\epsilon, \sigma)$ the simulated pressure of the state i using the parameter sets (ϵ, σ) for all different atom types.

To minimize the quantity $\mathcal{F}$, we use the well-known *Simplex* method [20], since this method does not involve derivative with respect parameters and can locate global minima, bypassing local minima that could restrict the optimization in general. Since the function to be minimized has no analytical derivative, using derivative methods one needs three simulations at each state point and iteration in order to calculate the value and the derivative of the function to be minimized, while using the Simplex method one needs $n+1$ simulations as starting point and then one simulation per state point and iteration, where n is the number of the parameters to be optimized. The location of the global minimum and the number of the required simulations is the advantage against the methods using derivatives described in Refs. [21,19]. This advantage is essential in the case of functional forms with many parameters. In Ref. [21] the quantity to be minimized is the sum of squared deviation of simulated quantity, divided by the squared statistical uncertainty of the quantity. This selection underestimates the contribution of state points that due to their nature have relatively high uncertainties and overestimates the contribution of state points with small uncertainties.

Finally, the original charges due to the Kinney's and Strauss's potentials as well as the bond and angle force parameters for the Olivet's model, have been kept constant during the optimization procedure of the other parameters. Partial charges, bond lengths, bond and angle constants can be obtained by quantum mechanics calculations.

For each PVT state point and intermolecular potential investigated here, an initial MD simulation was performed in NVT ensemble in order to equilibrate the system. Note that in each started simulation the potential parameters used are the original ones taken from the literature. Also, for each state point the initial MD run was extended for 1 ns with a time step of 1 fs. The initial configuration for all subsequent runs at each PVT point was the last saved configuration at this point. Each MD run spawned by the optimization procedure was extended to 50 ps to achieve equilibrium and subsequently 200 ps to estimate the pressure of the system. The Particle Mesh method was used to take into account long range electrostatic corrections for potential models that include charges, while in all cases the standard van der Waals long range corrections for potential energy and pressure were also applied. This makes the estimated potential parameters independent on the system size. In all MD simulations for force field optimization the number of molecules in the simulation box was 343, except the case of the spherical potential, where 1000 molecules were used. The cut-off distance used in each case was taken to be $6\sigma_F$ except for the simulation of the fluid with spherical potential where $6\sigma_{SF_6}$ was used. In all optimization simulations the Berendsen thermostat [22] was used with relaxation time of 0.2 ps and all degrees of freedom coupled. The shake algorithm was used to keep SF_6 molecules rigid for the rigid force fields. In all cases the resulting minimum of $\mathcal{F}$ from Eq. 3 was found to be in the range 0.0020–0.0023 (0.0020 for 7 sites, Strauss and Kinney, 0.0021 for Olivet and Pawley, and 0.0023 for spherical models). It means that the mean deviation of the predicted pressure from the experimental one is about 4.5%. All MD simulations were performed with GROMACS[23].

Minimization for each potential model needs 25–30 Simplex steps, depending on the starting parameters and potential form. We note that the optimization of the Olivet's potential, started with optimized Pawley's parameters, found no lower minimum for $\mathcal{F}$. Therefore, it is shown that according to this procedure both Pawley's and Olivet's optimized models exhibit the same Lennard Jones parameters for ϵ_F and σ_F. The optimized parameters obtained are summarized in Table 1 together with those corresponding to the original models. In addition, applying the same procedure we obtain a new rigid seven sites without charges potential and a spherical one for SF_6 treating the molecule as a single spherical site. By comparing the optimized with original parameters from Table 1, we may see that the most refined parameters with respect to the original values are those for σ, while the values for ϵ exhibit only a somewhat change in most cases.

4. Results and discussion

As mentioned above, the optimized force fields and the corresponding original ones are evaluated for their ability to predict results close to experimental data. It has been realized based upon experimental PVT diagram data, the liquid–gas coexistence curve, radial distribution functions, diffusion coefficient and shear viscosity.

4.1. PVT diagram

As usual, in the frame work of each MD simulation we have calculated the pressure, P, of the single phase fluid as a function of the molar volume, V_m, and temperature, T, for a number of different PVT thermodynamic state points. The length of the simulation of each state point of interest after equilibrium was 1 ns and the number of SF_6 molecules 750. In all MD simulations for the system properties estimation the Nose–Hoover [24,25] thermostat was used with a relaxation time of 0.2 ps and all the degrees of freedom coupled. The results are displayed in Fig. 1. In Fig. 2 we present the results for the new proposed spherical and seven sites without charges potential models. The corresponding values are presented in Table 5. From Fig. 1 and Table 5 we see that the original parameter set for all the force field forms investigated, are note accurate enough in description of the pressure in the PVT space under investigation. Concretely, Pawley's model overestimates the pressure of

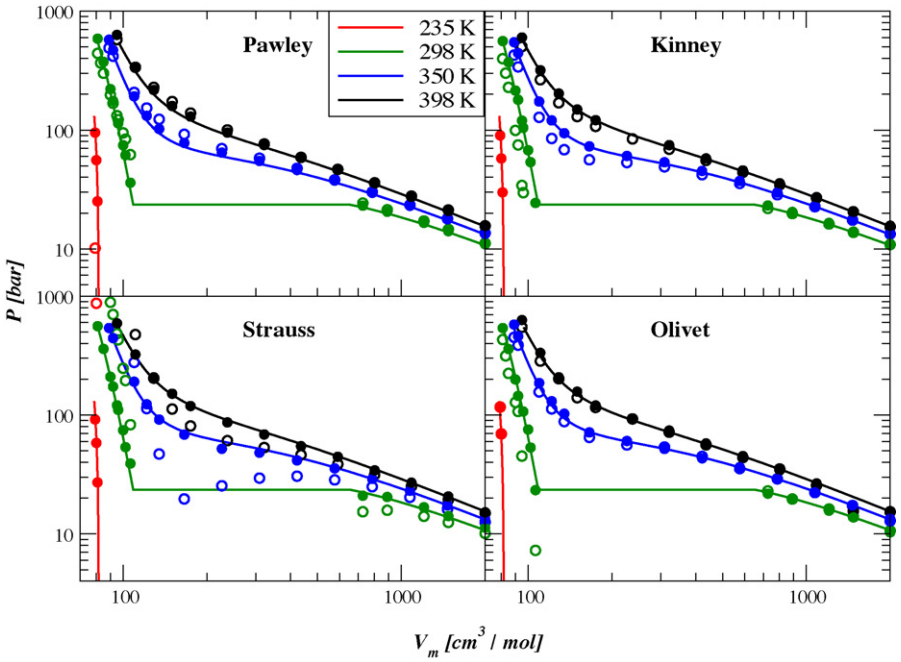

Fig. 1. The simulated and experimental PV diagram for isotherms 235 K (Liquid, red), 298 K (Liquid, vapor, green), 350 K (Supercritical, blue) and 398 K (Supercritical, black). Lines denote experimental [32], open circles the simulated using the original potential parameters and closed circles the simulated pressure using the optimized potential parameters. Missing points indicate either negative or extremely high pressure to include in graph. Both axes are in logarithmic scale. (For interpretation of the references to color in this figure legend, the reader is referred to the web version of the article.)

the fluid at medium densities, while at high densities underestimates this property. Kinney's model underestimates the pressure at all the examined temperatures and especially at medium as well as high densities. Strauss's model underestimates the pressure at low and medium densities while at high densities the results obtained show a significant overestimation. Especially at liquid state and for the isotherm $T = 235$ K, where the other existing potential models predict negative pressure, Strauss's model provides pressure more than 1000 bar. Finally, we found that the Olivet's six site flexible model, is the most accurate among the existing ones with regard to the pressure. Furthermore, our results have shown that this model exhibits relatively good values for pressure at low and medium densities, though a small but systematic overestimation appears at these densities. Note however that the aforementioned model underestimates the pressure at high densities and, on the other hand, predicts negative pressure in the whole density range at $T = 235$ K.

In Ref [19], the original Olivet potential was used to predict the density of homogeneous gas and liquid states using the NPT MD simulation technique. From Table IV in Ref. [19] it is easily seen that the Olivet potential exhibits deviation about 6% in the predicted density at the isotherm $T = 300$ K. The same state points were simulated in NPT ensemble using the new set of parameters for the Olivet force field. In our simulations, the Nose–Hoover thermostat [24,25] and Parrinelo–Rahman [26] barostat with relaxation time of 0.2 and 1.0 ps were used respectively. The number of molecules as well as other MD details, are the same with those mentioned above. The results from the employed NPT simulations are presented in Table 3 together with experiment and from Ref. [19]. From Table 3 we see that the deviation of the predicted density at 300 K using proposed parameters for Olivet potential of this work is less than 1% in all liquid states while the original parameters predict density deviation in range 4.9–6.3%.

In what follows here we shall limit the discussion to the results obtained for the pressure on the basis of the optimized parameter sets for all the potential functional forms used to simulate the fluid. To this point, we found that the use of these new parameter sets improve the ability of the models to predict results close to the experimental pressure.

From the results shown in Fig. 2 we may obtain that the seven sites model proposed in this work accurately predicts the experimental pressure at the state points under investigation. On the other hand, we see that the proposed spherical potential underestimates the pressure at high densities and temperatures. Its accuracy is similar to the original Pawley's potential model with the exception that the spherical potential predicts better results at the high density–low temperature region.

4.2. Potential energy

The accuracy of the original and optimized potential models has been also examined relatively to the potential interaction energy

Table 3
Comparison of the MD predicted density (ρ_{sim}) with experiment using the optimized flexible and the original Olivet model [19] for the homogenous gas and liquid states at 300 K. $\Delta\rho$ denotes the deviation of the MD predicted density from the corresponding experimental one.

P_{exp} [bar]	ρ_{exp} [g/cm^3]	ρ_{sim}^{orig} [g/cm^3]	ρ_{sim}^{opt}	$\Delta\rho_{orig}$ (%)	$\Delta\rho_{opt}$ (%)
5.01	0.031149	0.0329±0.012	0.03211±0.001	5.6	3.0
20.03	0.162945	0.161±0.012	0.1628±0.007	1.2	0.09
40.14	1.382802	1.47±0.05	1.3947±0.02	6.3	0.8
60.17	1.435524	1.52±0.04	1.4381±0.04	5.9	0.2
80.18	1.474228	1.55±0.04	1.4674±0.02	5.1	0.4
100.19	1.505417	1.58±0.04	1.5168±0.02	4.9	0.7

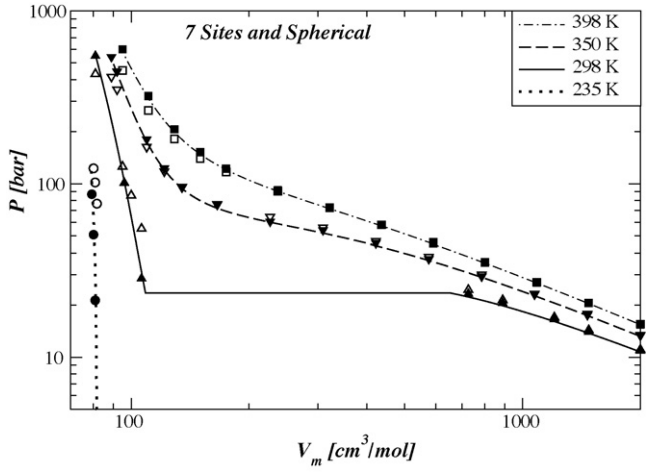

Fig. 2. The simulated pressure using the spherical (open symbols) and seven sites without charges (closed symbols) models and experimental [32] (lines) PV diagram for isotherms 235, 298, 350 and 398 K. Both axes are in logarithmic scale.

they predict as a function of the molar volume. The results obtained at the isotherm $T = 350$ K are presented in Fig. 3 and Table 5. From Fig. 3 and Table 5 it is easily seen that all potential models, except the original Pawley's and Strauss's ones, predict values for potential energy that are very close to each other. Concretely, the original Pawley's model predicts weaker interaction while that of Strauss stronger. Note that, to our knowledge, experimental values of potential energy are not available in the literature. The values presented in Table 5 are just a test of how close is the predicted potential energy by the potential models under investigation.

4.3. Liquid–vapour coexistence

As mentioned above, it is found that the optimized potentials adequately predict the experimental pressure in the PVT state points under investigation, that cover almost the whole area where experimental data are available, while the existing potential models from the literature do not sufficiently describe the low temperature–high density region. In what follows, we shall present results obtained on the basis of these potentials concerning certain properties of the fluid.

The property we examined here is the liquid–vapor coexistence or in other words, the ability of the refined potentials to predict successfully the liquid-vapor coexistence density envelope. One may predict points along the liquid–vapor coexistence curve by using the Gibbs Ensemble Monte Carlo (GEMC) technique [27] or alternatively Molecular Dynamics simulation as in previous studies of SF_6[19,18]. GEMC is the method that fits better this kind of calculations since pressure calculation is trial while with the elongated box MD method there are various issues to be taken into account, like the identification of the gas and liquid regions. In order to compare the two methods, we performed both kinds of calculations for the optimized Pawley's model. The GEMC procedure is standard [27]. The Molecular Dynamics method described in [19,18] and references therein, puts a liquid phase into an one dimension expanded box and leaves the system to evolve increasing the temperature.

In previous studies, the simulation box has four times higher volume than that of the liquid. In this study, we use the method described in [19,18] with the following modification : We equilibrate SF_6 at low temperature and experimental density and then we expand the one dimension of the box. The expanded dimension is such as the volume of the elongated box reproduces the critical density. This results in a box with the one dimension 2.44 times the dimension of the cubic box of SF_6 at 230 K instead of 4 times used in [19,18]. Following the same procedure and MD computational details as in previous studies [19,18], we find the density profile along the elongated dimension axis at each temperature. The results from this Molecular Dynamics study for the optimized Pawley's potential model are presented in Fig. 4.

In the GEMC calculations, we use 432 SF_6 molecules, by performing composite translation/rotation, volume exchange and inter-box molecule transfer moves, with relative probability 9990:9:1 respectively for 10^7 moves. For each PVT state point of interest, an initial equilibration run of 10^6 steps with only translation/rotation moves was performed for the two boxes with dimensions corresponding to experimental liquid and vapor densities, respectively. Then the GEMC method was used with this configuration as an initial one. All Monte Carlo calculations were performed with the Towhee package [28]. The liquid and vapor densities obtained as well as their corresponding uncertainties are presented in Fig. 4 for the optimized Pawley's potential model. It is obvious from the results in Fig. 4 that both methods are almost equivalent.

From the GEMC data, we may estimate the critical parameters of SF_6, namely the critical temperature T_c and density ρ_c using the rectilinear diameter law and compare with experimental data

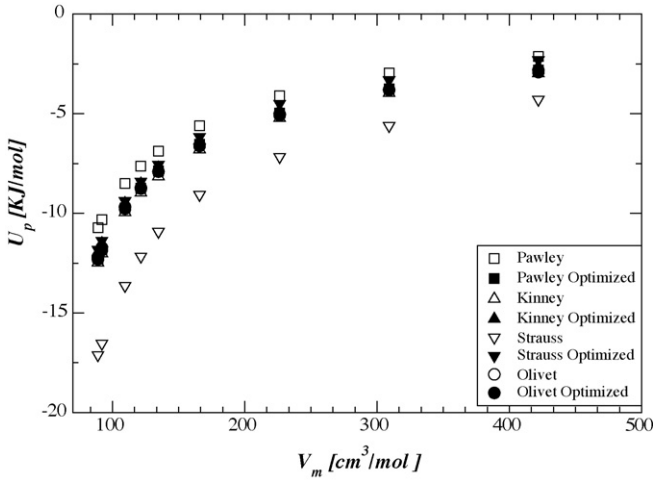

Fig. 3. The simulated potential energy of the SF_6 fluid as function of molecular volume at 350 K.

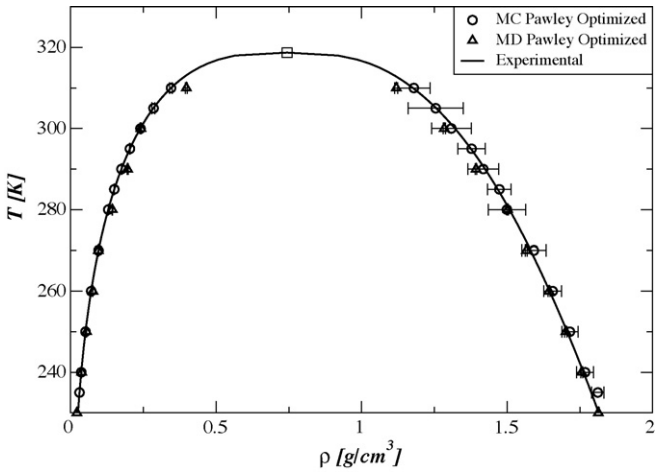

Fig. 4. Comparison of the coexistence envelope for SF_6 for the optimized Pawley model predicted by the elongated box MD and GEMC calculations. Line corresponds to experimental data [32], circles to the GEMC and triangles to the elongated box Molecular Dynamics Simulation results, respectively.

Table 4
The predicted critical parameters of SF_6 using GEMC simulation for the optimized potentials.

	T_c [K]	ρ_c [g/cm^3]	P_c [bar]	β
Experimental [32]	318.73	0.7438	37.5	
Pawley optimized	318.16	0.7400	39.3	0.3278
Kinney optimized	317.92	0.7453	39.8	0.3126
Strauss optimized	317.94	0.7452	39.8	0.3159
7 sites	317.13	0.7485	38.2	0.3256
Spherical	308.47	0.6952	33.3	0.2967

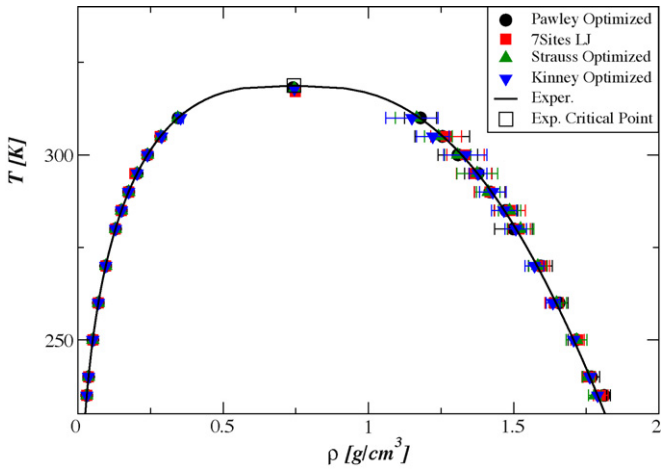

Fig. 5. The liquid–vapor coexistence envelope for SF_6 for the optimized models. Line corresponds to experimental data [32], circles to the GEMC results, respectively.

[18,29–31]:

$$\frac{\rho_\ell + \rho_v}{2} = \rho_c + C(T_c - T) \tag{4}$$

$$\rho_\ell - \rho_v = B_0(T_c - T)^\beta + B_1(T_c - T)^{\beta+\Delta} + B_2(T_c - T)^{\beta+2\Delta} + \cdots \tag{5}$$

The resulting parameters of the fitted Eqs. (4) and (5) to the (T, ρ) GEMC data are presented in Table 4. The corresponding coexistence envelopes from GEMC calculations are presented in Fig. 5 note that the fitting Eq. (5) was constrained to the first term due to the fact that the fitted values for parameters B_1 and B_2 found to be very small resulting the large uncertainty for parameter Δ.

From the data in Table 4, it is clearly seen that all the site–site potential models, optimized using the method described in previous section, accurately predict the critical temperature T_c and density ρ_c of the SF_6 fluid. Note that the deviation of the results obtained with respect to the experimental values [32] is about 0.6% that is sufficiently better than the deviation reported in previous treatments, namely 2.5% for T_c and 2.8% for ρ_c in Ref. [19] and 9% for T_c and 13% for ρ_c in Ref. [18]. Finally, in the case of the one site spherical potential, we found that the proposed potential model predicts much better the experimental critical parameters of the fluid compared to the original six site Pawley's potential, though it exhibits a deviation from the experimental values 3% for T_c and 6.5% for ρ_c. It is not however adequate in predicting these parameters when compared with the other site–site optimized potentials.

The GEMC predicted vapor pressure as function of temperature for the optimized models as well as the corresponding experimental data are presented in Fig. 6. The vapor pressure was fitted to Claussius–Clapeyron equation:

$$P_v = Ae^{-(\Delta H_{vap}/RT)} \tag{6}$$

Using the fitted parameters A, ΔH_{vap} and the previously fitted critical temperature T_c, we obtain the critical pressure P_c. The obtained critical pressure for the optimized models is also presented in Table 4.

4.4. Structural properties

The structural properties predicted by the original and optimized potential models were explored on the basis of the site–site radial distribution functions (rdfs). In the experimental work of the Strauss [13] the total rdf is given by the weighted sum of the site–site rdfs, namely:

$$g_{total}(r) = 0.006g_{SS}(r) + 0.143g_{SF}(r) + 0.851g_{FF}(r) \tag{7}$$

In the framework of this study, we calculated the site–site rdfs for each potential model under investigation. Further to this and

Table 5
The simulated potential energy at 350 K for the original and optimized force fields.

V_m [cm^3/mol]	$-U_p$ [kJ/mol]				
	Pawley		Kinney		Spherical
	Orig.	Optim.	Orig.	Optim.	
421.90	2.120±0.069	2.812±0.096	2.978±0.107	2.634±0.089	2.106±0.064
309.06	2.958±0.078	3.744±0.099	3.965±0.129	3.617±0.107	2.824±0.071
226.40	4.094±0.094	4.961±0.118	5.222±0.127	4.820±0.106	3.754±0.076
165.85	5.606±0.091	6.537±0.108	6.791±0.128	6.355±0.089	4.957±0.074
134.77	6.880±0.091	7.874±0.096	8.150±0.102	7.719±0.086	5.989±0.071
121.49	7.634±0.086	8.737±0.093	8.969±0.096	8.518±0.080	6.598±0.070
109.52	8.499±0.080	9.736±0.089	9.948±0.088	9.502±0.082	7.285±0.070
92.00	10.323±0.079	11.832±0.083	12.017±0.082	11.511±0.081	8.615±0.077
89.00	10.730±0.079	12.302±0.083	12.475±0.082	11.956±0.082	8.887±0.079
	Strauss		Olivet		7 sites
	Orig.	Optim.	Orig.	Optim.	
421.90	4.291±0.178	2.307±0.072	2.819±0.081	2.913±0.095	2.695±0.098
309.06	5.611±0.159	3.312±0.085	3.788±0.105	3.811±0.123	3.629±0.113
226.40	7.166±0.188	4.497±0.095	5.077±0.114	5.021±0.105	4.899±0.114
165.85	9.069±0.136	6.161±0.089	6.583±0.110	6.622±0.095	6.406±0.102
134.77	10.921±0.088	7.552±0.098	7.910±0.107	7.905±0.106	7.765±0.088
121.49	12.165±0.085	8.400±0.088	8.718±0.096	8.759±0.092	8.596±0.085
109.52	13.637±0.083	9.379±0.082	9.683±0.094	9.764±0.084	9.571±0.086
92.00	16.534±0.097	11.371±0.083	11.715±0.087	11.847±0.083	11.601±0.083
89.00	17.109±0.099	11.819±0.082	12.182±0.082	12.309±0.086	12.043±0.083

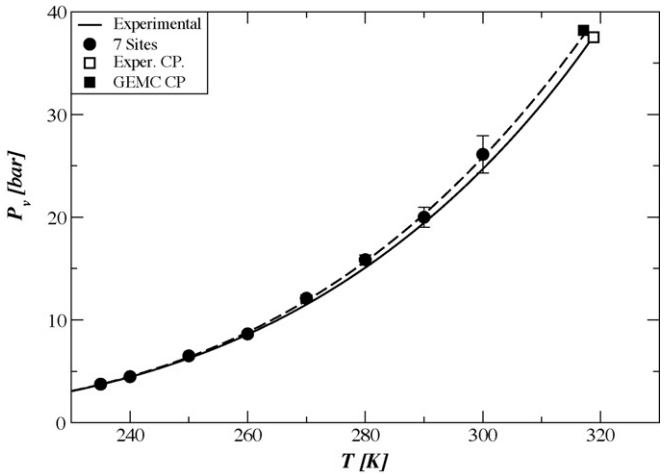

Fig. 6. Experimental and MD predicted by the 7 site model of this work vapor P–T diagram for SF_6. Solid line represent the experimental pressure [32], filled circles the GEMC points, dashed line the Claussius–Clapeyron fit. Filled square is the predicted by the model and open square the experimental critical point.

according to Eq. (7), we calculated the total rdf, at the state points where experimental data are available [13]. The MD simulations for the calculation of the rdfs were extended up to 1 ns using 750 SF_6 molecules. The simulated total rdf, at 398 K and density 1.85 g/cm^3 for both the original and optimized potential parameters is displayed in Fig. 7.

From the results in Fig. 7 it seems that the total rdfs, as well as the site–site ones not shown separately here, predicted by the potential models are very close to each other. The comparison of the simulated and experimental total rdfs shows that the predicted shape is quite similar. The shoulder at short correlation distance is reproduced with a slightly different shape shifted somewhat towards lower position. In addition, the rest of the peaks are accurately predicted both in location and shape. Let us now consider the efficiency of the original Strauss's potential, in reproducing the structure of the fluid. So, from the results in Fig. 7 we have to mention that this potential exhibits a systematic deviation of the predicting peaks compared with experiment. It is easily seen that the peaks of the rdf are shifted towards higher correlation distances and therefore fails to describe accurately the experimental rdf data [13].

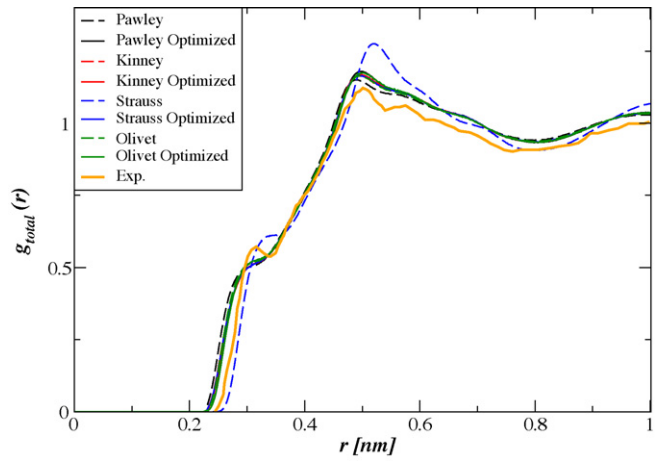

Fig. 7. The simulated and experimental [13] total radial distribution functions of SF_6 at 398 K and density 1.85 g/cm^3.

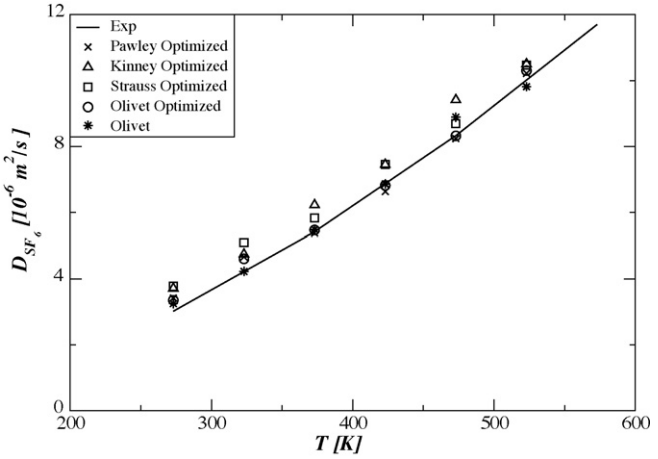

Fig. 8. Comparison of the experimental [33] and predicted self-diffusion coefficient of SF_6 at atmospheric pressure using the optimized and original Olivet's potential models.

4.5. Self-diffusion coefficient

In their previous MD treatment, Olivet et al. [19,18] reported the temperature dependence of the self-diffusion coefficients of SF_6 in contrast to the corresponding experimental values at atmospheric pressure [33]. In the present study, the self-diffusion coefficients of the species were recalculated from the MD trajectories based on the optimized and original Olivet's potential model by using the well-known Einstein relation:

$$D = \frac{1}{6t}\langle|\vec{r}_i(t) - \vec{r}_i(0)|^2\rangle \quad (8)$$

Note that the simulations of the fluid at atmospheric pressure (i.e. very low density fluid) were carried out specifically with 1000 SF_6 molecules to achieve better statistics. In addition, these MD runs were performed in the NVE ensemble, extended up to 4 ns after the initial equilibration period of 1 ns. The self-diffusion coefficients obtained for all the optimized potential models are presented in Fig. 8 together with available experimental values [33].

From the data presented in Fig 8, we see that all the predicted diffusion coefficients by the models used is only few per cent far from the experimental one. In other words, we do not find significant differences among the predicted self-diffusion coefficients of the aforementioned models, a result that led us to conclude that the simulation of this transport property is not strongly affected by the potential model used, for densities corresponding to atmospheric pressure. In Ref. [1] the experimental self-diffusion coefficient of SF_6 is reported for high densities at liquid and supercritical states. The original Pawley model was used in MD simulation of self-diffusion coefficient at these states in Ref. [10]. The self-diffusion coefficient was calculated at these dense states using the new proposed potential parameters. The results are presented in Table 6.

4.6. Shear viscosity

Shear viscosity is a good force field validation property. Thus, the shear viscosity of SF_6 was calculated at the 333.15 K isotherm, where experimental [34] and previously reported simulated values [19] are available. In these simulations 216 SF_6 molecules were used in the NVE ensemble. The simulations were extended up to 10 ns. The momentum fluctuations method [35,36] was used to calculate this property. The values of shear viscosity obtained are presented in Table 7. As it can be seen from the values in Table 7, the optimized force fields predict shear viscosity with deviation less than 10% from

Table 6
The experimental [1] and simulated self-diffusion coefficient of SF_6 at relatively high densities.

T [K]	ρ [g/cm^{-3}]	P_{exp} [bar]	D_{exp} [10^{-5} cm^2/s]	T_{sim} [K]	P_{sim} [bar]	D_{sim} [10^{-5} cm^2/s]
			7 sites			
398	1.30	298	15.40	398.5±4	303±71	13.36±0.20
398	1.85	1544	4.94	399.1±4	1588±140	4.91±0.21
296	1.50	84	7.70	295.7±3	76±63.5	7.18±0.20
296	1.90	1167	2.32	296.2±3	858±116	2.65±0.12
			Olivet			
398	1.30	298	15.40	399.1±5	285±328	13.35±0.04
398	1.85	1544	4.94	399.3±6	1384±450	4.36±0.01
296	1.50	84	7.70	298.9±3	21±341	7.08±0.16
296	1.90	1167	2.32	298.8±4	658±410	2.86±0.09
			Olivet optimized			
398	1.30	298	15.40	395.3±3	289±316	13.84±0.02
398	1.85	1544	4.94	400.3±3	1615±465	4.31±0.03
296	1.50	84	7.70	298.6±3	99.5±324	7.16±0.10
296	1.90	1167	2.32	297.7±2	955±434	2.43±0.08

Table 7
The experimental [34] and simulated shear viscosity of SF_6 at 333.15 K from this work and previous study [19].

P_{exp} [34] [P_{bar}]	P_{sim}	η_{exp} [34] [μ Pa s]	η_{sim}	$\Delta\eta$ (%)
		Pawley		
50.00	70.24	41.89	38.12±0.37	−9.0
69.51	102.27	79.52	70.33±0.26	−11.5
91.06	125.79	97.95	88.85±1.21	−9.3
104.65	137.63	106.74	93.15±0.86	−12.7
		Olivet [19]		
50.00	50.75	41.89	63±6	50.4
69.51	77.20	79.52	88±7	10.7
91.06	83.91	97.95	102±7	4.1
104.65	105.13	106.74	115±8	7.8
		Olivet opt.		
50.00	52.7	41.89	39.30±0.33	−6.2
69.51	67.84	79.52	71.62±0.33	−9.9
91.06	89.70	97.95	94.65±0.54	−3.4
104.65	110.69	106.74	104.62±0.89	−1.9
		Strauss opt.		
50.00	53.31	41.89	37.71±0.32	−9.9
69.51	72.02	79.52	76.41±1.29	−3.9
91.06	96.14	97.95	90.79±0.49	−7.3
104.65	109.60	106.74	100.36±1.01	−6.0
		7LJ		
50.00	50.05	41.89	39.41±0.71	−5.9
69.51	69.04	79.52	77.96±0.99	−2.0
91.06	89.49	97.95	89.61±0.61	−8.5
104.65	104.58	106.74	101.81±1.54	−4.6

experimental values at this isotherm. This result also reveals the reliability of the proposed force field parameters.

5. Conclusions

The main purpose of this MD study has been to investigate the accuracy of few common forms of effective potential models available in the literature for the SF_6 fluid and to propose, when needed, optimized parameters of them to predict properties of the system close to the experimental data. According to the literature, among others, four common different functional forms for the intermolecular interaction potential of the SF_6 fluid have been reported so far. To realize our aim we employed an optimization procedure that optimizes the Lennard–Jones parameters to experimental pressure at four different isotherms, namely one characterizing the pure liquid at low temperature, one the supercritical fluid at high temperature and the rest two being close (one below and one above) to the critical temperature. Further to this, and based on the same optimization procedure we also propose a spherical, single interaction site potential model that might be useful in pure theoretical studies as well as a rigid seven sites one without electrostatic interactions.

The evaluation of all the previously reported and in this study optimized potential models of SF_6 led us to conclude about their ability to predict successfully experimental properties. Thus, we found that the available from literature potential models do not accurately predict the experimental pressure especially at low temperature–high density states region. On the other hand, the effectiveness of the optimized models to adequately approximate this property in a wide range of thermodynamic state points, where experimental data are available, has been sufficiently verified.

In the case of the potential energy, the results obtained reveal that all the potential models explored, except the original Pawley's and Strauss's ones, predict values that are very close to each other.

Using the above mentioned potential models with optimized parameters we performed GEMC simulations in order to estimate the critical temperature and density of SF_6. The predicted critical properties are found in excellent agreement with experimental values. We obtained the critical temperature in the range 317.13–318.16 K that is quite close to the experimental one

(T_c =318.73 K) and density in the range 0.7400–0.7485 with an experimental value of 0.7438 g/cm^3. Note that the original Pawley's and Olivet's potentials predicted critical temperature 345.887, 310.7 K and density 0.659, 0.76 g/cm^3, respectively [19,18].

The intermolecular structure of the molecular system predicted by the original and optimized potential models was explored on the basis of the calculated appropriate site–site rdfs. In each case from the corresponding site–site rdfs we obtained the total rdf as the weighted sum of these functions. We also calculated the total rdfs at the state points where experimental data are available. We found that all the site–site potential models, except the original Strauss model, predict almost the same shape and location of maxima and minima of the total rdfs. As a general outcome, it is found that the predicted total rdfs exhibit almost the same features as the experimental ones, except their behavior at very short correlation distances.

The calculated self-diffusion coefficients of the fluid predicted on the basis of the optimized models are very close to experimental values at atmospheric pressure and temperature in the range 273–523 K, as well as at the isotherms of 296 and 398 K. The values due to the Strauss's and Kinney's optimized models are somewhat overestimated. The calculated shear viscosity predicted by the optimized force field parameters are in better agreement with experimental values compared to those obtained using the original parameters, at least at states where experimental data are available.

Finally, we may conclude that for some common functional forms of these force fields, the newly optimized parameters predict better the experimental properties of SF_6 under investigation compared to the original model.

References

[1] J. Dezwaan, J. Jonas, J. Chem. Phys. 63 (1975) 4606.
[2] H.A. Posch, T.A. Litovitz, Mol. Phys. 32 (1976) 1559.
[3] G. Pawley, Mol. Phys. 43 (1981) 1321.
[4] M.T. Dove, G.S. Pawley, J. Phys. Lett. 48 (1982) 410.
[5] J.G. Powles, J.C. Dore, M.B. Deraman, E.K. Osae, Mol. Phys. 50 (1983) 1089.
[6] M.T. Dove, G.S. Pawley, J. Phys. C: Solid State Phys. 16 (1983) 5969.
[7] M.T. Dove, G.S. Pawley, J. Phys. C: Solid State Phys. 17 (1984) 6581.
[8] B.M. Powell, M.T. Dove, G.S. Pawley, L.S. Bartell, Mol. Phys. 62 (1987) 1127.
[9] C. Hoheisel, Int. J. Thermophys. 10 (1989) 101.
[10] A. Brodka, T.W. Zerda, Mol. Phys. 76 (1992) 103.
[11] F.M. Beniere, A. Boutin, J. Simon, A.H. Fuchs, M.F. de Feraudy, G. Torchet, J. Phys. Chem. 97 (1993) 10472.
[12] A. Boutin, B. Rousseau, A.H. Fuchs, Chem. Phys. Lett. 218 (1994) 122.
[13] G. Strauss, H. Zweier, H. Bertagnolli, T. Bausenwein, K. Tödheide, P. Chieux, J. Chem. Phys. 101 (1994) 662.
[14] K.E. Kinney, S. Xu, L.S. Bartell, J. Phys. Chem. 100 (1996) 6935.
[15] S. Tanimura, K. Yasuoka, T. Ebisuzaki, J. Chem. Phys. 109 (1998) 4492.
[16] C. Moon, G.S. Pawley, J. Mol. Struct. 486–486 (1999) 479.
[17] F. Gámez, S. Lago, F. del Rio, A.L. Benavides, J. Chem. Phys. 125 (2006) 104505.
[18] A. Olivet, D. Duque, L.F. Vega, J. Chem. Phys. 123 (2005) 194508.
[19] A. Olivet, L.F. Vega, J. Chem. Phys. 126 (2007) 144502.
[20] J. Nelder, R. Mead, Comput. J. 7 (1965) 308.
[21] P. Ungerer, C. Beauvais, J. Delhommelle, A. Boutin, B. Rousseau, A.H. Fuchs, J. Chem. Phys. 112 (2000) 5499.
[22] H.J.C. Berendsen, J.P.M. Postma, A. DiNola, J.R.J. Haak, Chem. Phys. 81 (1984) 3684.
[23] B. Hess, C. Kutzner, D. van der Spoel, E. Lindahl, J. Chem. Theory Comput. 4 (2008) 435.
[24] S. Nosé, Mol. Phys. 52 (1984) 255.
[25] W.G. Hoover, Phys. Rev. A 31 (1985) 1695.
[26] M. Parrinello, A. Rahman, J. Appl. Phys. 52 (1981) 7182–7190.
[27] A.Z. Panagiotopoulos, Mol. Phys. 61 (1987) 813.
[28] Available at http://towhee.sourceforge.net.
[29] F.J. Wegner, Phys. Rev. 54 (1975) 1.
[30] K. Riedel, F.J. Wegner, Phys. Rev. 9 (1974) 294.
[31] F.J. Wegner, Phys. Rev. 5 (1972) 4529.
[32] E.W. Lemmon, M. McLinden, D. Friend, Thermophysical Properties of Fluid Systems in NIST Chemistry WebBook, NIST Standard Reference Database Number 69, In: P.J. Linstrom, W.G. Mallard (Eds.), National Institute of Standards and Technology, Gaithersburg, MD, 20899 (http://webbook.nist.gov), June 2005.
[33] A. Boushehri, J. Bzowski, J. Kestin, A. Mason, J. Phys. Chem. Ref. Data 16 (1987) 445.
[34] J. Wilhelm, D. Seibt, E. Bich, E. Vogel, E. Hassel, J. Chem. Eng. Data 50 (2005) 896.
[35] B.J. Palmer, Phys. Rev. E 49 (1994) 359.
[36] B. Hess, J. Chem. Phys. 116 (2002) 209.